HHS Public Access

Author manuscript

Drug Deliv Transl Res. Author manuscript; available in PMC 2019 June 01.

Published in final edited form as:

Drug Deliv Transl Res. 2018 June ; 8(3): 843–852. doi:10.1007/s13346-018-0495-7.

Full Depth Measurement of Tenofovir Transport in Rectal Mucosa using Confocal Raman Spectroscopy and Optical Coherence Tomography

Aubrey L. Presnell[1], **Oranat Chuchuen**[2,3], **Morgan G. Simmons**[1], **Jason R. Maher**[1], and **David F. Katz**[1,4,*]

[1]Department of Biomedical Engineering, Duke University, Durham, North Carolina 27708

[2]Department of Biotechnology, Faculty of Technology, Khon Kaen University, Khon Kaen, Thailand 40002

[3]Mekong Health Science Research Institute, Khon Kaen University, Khon Kaen, Thailand 40002

[4]Department of Obstetrics and Gynecology, Duke University, Durham, North Carolina 27708

Abstract

The prophylactic activity of antiretroviral drugs applied as microbicides against sexually transmitted HIV is dependent upon their concentrations in infectable host cells. Within mucosal sites of infection (e.g. vaginal and rectal mucosa), those cells exist primarily in the stromal layer of the tissue. Traditional pharmacokinetic studies of these drugs have been challenged by poor temporal and spatial specificity. Newer techniques to measure drug concentrations, involving Raman spectroscopy, have been limited by laser penetration depth into tissue. Utilizing confocal Raman spectroscopy (RS) in conjunction with optical coherence tomography (OCT), a new lateral imaging assay enabled concentration distributions to be imaged with spatial and temporal specificity throughout the full depth of a tissue specimen. The new methodology was applied in rectal tissue using a clinical rectal gel formulation of 1% Tenofovir (TFV). Confocal RS revealed diffusion-like behavior of TFV through the tissue specimen, with significant partitioning of the drug at the interface between the stromal and adipose tissue layers. This has implications for drug delivery to infectable tissue sites. The new assay can be applied to rigorously analyze microbicide transport and delineate fundamental transport parameters of the drugs (released from a variety of delivery vehicles) throughout the mucosa, thus informing microbicide product design.

Keywords

microbicides; Tenofovir; rectal mucosa; Raman spectroscopy; optical coherence tomography; drug delivery

[*]Corresponding author: David Katz; Room 1391 CIEMAS; 101 Science Dr., Box 90281; Durham, North Carolina 27708, dkatz@duke.edu | Phone: (919) 660-5452.

Conflicts of Interest

The authors declare that they have no conflicts of interest, including no conflicting financial relationships with the National Institutes of Health, which sponsored this research under grant AI13127.

Introduction

Many drugs are applied topically for local activity in mucosal tissue. Microbicide drugs and products are currently being developed for activity in preventing infection by sexually transmitted HIV and other pathogens within the vaginal and rectal mucosa[1]. Notably, exposure of the rectal mucosa to sexually transmitted HIV has a higher likelihood of infection than exposure of the vaginal mucosa[2–4]. Rational design and performance evaluation of microbicides benefit from objective understanding of the determinants of the pharmacokinetics (PK) achieved by candidate products[5, 6]. This understanding informs choices in drug vehicle design and loading and in determining optimal dosage regimens. Further, it can guide choices in the design and interpretation of PK studies – for example, optimal sampling times to capture the time dependence of drug transport and details of drug concentration measurements within sampled mucosal tissue (e.g. in biopsies)[6–9].

Drug transport from a vehicle inserted into the vaginal or rectal lumens ‘down’ into the mucosa is a transport process that is diffusional or diffusion-like[10]. Drug concentration is not uniformly distributed with respect to depth in the tissue, and it varies temporally, as well. This spatiotemporal variability challenges measurements of drug concentrations in biopsy specimens; those measurements are traditionally performed by first homogenizing the tissue and then attaining mass-averaged concentrations by analytical methods such as HPLC or LC-MS/MS[11–14]. Such mass averages do not capture partitioning of drug between structurally different layers in the mucosa, i.e. the epithelium and stroma (lamina propria)[7, 8, 15, 16]. The human vaginal mucosa has a stratified squamous epithelium that varies in thickness from about 150 – 200 μm, depending upon factors such as the phase of the menstrual cycle[17]. The human vaginal stroma is about 3 mm thick, and is comprised primarily of connective tissue, with small concentrations of cells, a vasculature, and lymphatics[18]. The rectal mucosa has a very different structure. The epithelium consists of a single columnar layer of cells about 25 μm thick that is configured around crypts which penetrate into the stroma[19]. That stroma is about 1 mm thick, and is comprised of connective tissue, vasculature, plasma cells, and lymphocytes; beneath it is a lipid layer that lies above the submucosa. Cells in the stroma are a primary site of infection by sexually transmitted HIV, as this layer houses a host of infectable immune cells including macrophages, dendritic cells, and $CD4^+$ T cells. Depending upon the physicochemical properties of the drug (e.g. hydrophilic vs. hydrophobic/lipophilic) and the target mucosa (vaginal or rectal), as well as the thicknesses of biopsies, mass averaged concentrations within the biopsies may overestimate or underestimate drug concentrations within the stroma, where antiretroviral drugs primarily act against HIV[7, 8].

Other methods exist which could enable determination of spatially varying concentration profiles. HPLC or LC-MS/MS can be used in combination with tissue sectioning to produce a spatial map of drug concentrations throughout the tissue[20]. However, such sectioning-based techniques depend upon the precision of the sectioning method, necessitate destruction of a specimen during analysis, and do not account for temporal variations in concentration. Sample-to-sample variability of tissue also frustrates attempts to identify meaningful differences in concentrations at different depths or to compare samples between different time points. Non-invasive techniques are appealing in that the integrity of the tissue

can be maintained. Attenuated total reflection Fourier transform infrared spectroscopy (ATR-FTIR) is one such method and has been used in studies of drug diffusion, particularly for dermal applications[21]. When combined with tape-stripping or tissue-sectioning, it can provide a sensitive map of concentration within different layers. However, the strong absorbance of water in the IR region prevents the analysis of hydrated tissue samples using this technique. Alternatively, Raman spectroscopy, the technique employed in this study, is ideally suited for hydrated samples since water is a weak Raman scatterer. Raman also provides more spatial and spectral specificity when compared with IR techniques, making it an especially attractive method for analyzing the distribution of drugs within the target mucosa.

Fundamental to mechanistic understanding of microbicide drug pharmacokinetics is knowledge of salient drug transport parameters within the vehicle and host environment – e.g. the diffusion and partition coefficients for all compartments in the system (e.g. vehicle, epithelium, stroma). These have intrinsic value in interpreting and comparing rates of drug transport, more so than the traditional permeability parameter which is a tissue volume-averaged parameter related to both the diffusion and partition coefficients throughout a specimen[22]. The diffusion and partition coefficients are also key inputs to deterministic, computational compartmental modeling of PK, which informs both fundamental understanding of drug delivery and its application in product design and performance evaluation[5, 6].

Previously, we introduced and applied confocal Raman spectroscopy (RS) and optical coherence tomography (OCT) to analyze microbicide diffusion into mucosal tissue[10, 16]. First, we developed and described a basic method for applying Raman to obtain drug concentration profiles[10, 16]. Then, we improved the methodology technically and applied it to obtain diffusion and partition coefficients of the non-nucleotide reverse transcriptase inhibiting drug, tenofovir (TFV), in a gel vehicle[22] and in the epithelial and stromal layers of vaginal mucosal tissue[23]. Tenofovir is a primary anti-HIV drug that is used orally for both HIV infection therapy and prevention[24]. It is currently being evaluated for topical application for HIV prophylaxis[25]. Our previous methodology employed confocal Raman imaging, co-registered with OCT, in a configuration in which the imaging beam focused ‘down’ through the layers of vehicle and excised mucosal tissue, i.e. ‘z-scans’. Such scanning is challenged by light scattering as the plane of focus is moved deeper into the tissue. The practical scanning depth is about 300 μm below the surface, which is approximately equal to the transport length or reduced mean free path of near-infrared light in the tissue[16]. Since the thickness of the stroma and its depth below the mucosal surface can be much greater than this distance, there is considerable motivation to create and apply a method for measuring drug concentrations at such depths. Here, we introduce such a method. The imaging beam now strikes the tissue from the side, rather than the apical surface of a specimen, which we refer to as “lateral.” The confocal imaging plane is fixed, and the tissue specimen is mechanically moved left and right relative to the imaging beam. This creates a scan in the normal direction with respect to the epithelial surface, at a fixed depth from the lateral edge. In the study here, we have applied the method to specimens of excised porcine rectal tissue to measure drug concentrations at increased depths below the

epithelial surface. We again utilized tenofovir as the target molecule with which to implement the methodology.

Materials and Methods

A. Materials

Porcine rectal tissue was harvested from pigs obtained from a local abattoir immediately after slaughter (Hatley Family Farms, Hurdle Mills, NC). Tissue was transferred to the lab in ice-cold, modified Krebs buffer (115 mM NaCl, 2.4 mM K_2HPO_4, 0.4 mM KH_2PO_4, 1.2 mM $CaCl_2$, 1.2 mM $MgCl_2$, 25 mM $NaHCO_3$, bubbled with carbogen) formulated to a pH of 7.3–7.4 to more closely match the environment in the rectum[26]. Surgical scissors were used to remove excess fat, muscle, and connective tissue external to the mucosa. Excised tissue samples (~3×3 cm) were then cleaned with modified Krebs buffer, snap frozen in liquid nitrogen, and stored at −80°C prior to analysis.

Pure tenofovir (TFV) was kindly provided by the CONRAD program (Arlington, VA). TFV rectal gel and matched placebo gel used in these experiments were kindly provided by Professor Lisa C. Rohan (University of Pittsburgh, School of Pharmacy). The gel was formulated with 1% TFV as well as Carbopol® 947P NF, sodium carboxymethylcellulose, methyl paraben, propyl paraben, glycerol, edetate disodium (EDTA), sodium hydroxide, and purified water. This was the same rectal specific microbicide formulation used in the CHARM-01 and CHARM-02 rectal microbicide studies[3, 27, 28].

B. Histology

Samples of rectal mucosa (~2.5×5 cm) positioned at different locations 0 to 25 cm proximal to the anal sphincter were excised for histological analysis. Standard hematoxylin & eosin staining and interpretation were performed by the Histopathology Core at the Duke School of Medicine, Department of Surgery. Interpretation was provided by a pathologist, Dr. Jeffrey Everitt, in the Animal Pathology Core at Duke University, Department of Pathology.

C. Raman Spectral Acquisition

All Raman spectra were acquired on a custom built confocal Raman system with co-registered optical coherence tomography (RS-OCT)[16]. The confocal RS subsystem utilizes a 785-nm laser diode (LD785-SH300, Thorlabs Inc., Newton, NJ) that delivers approximately 38 mW of power to the sample plane. A water immersion objective (W Plan-Apochromat 40x/1.0, Carl Zeiss Microscopy, LLC, Thornwood, NY) was used, which yields high axial and lateral resolutions of 11 μm and 5.5 μm respectively for the confocal RS subsystem. The OCT subsystem has axial and lateral resolutions of 6 μm and 44 μm, respectively, with a lateral field of view of 530 μm. Thus, drug distribution and tissue morphology can be imaged and analyzed with sub-100 μm resolutions. Axial and lateral resolutions were quantified using a protocol defined previously[16].

Additionally, the confocal RS-OCT setup includes a temperature-controlled, motorized stage, allowing the sample to be maintained at physiological temperature (37°C) throughout the duration of experiments. Motorized translation of the stage was controlled with custom

software written in LabVIEW (National Instruments, Austin, TX), enabling data to be collected from precise locations within the tissue sample. All raw spectra were processed using a custom MATLAB script that has been described previously[16].

D. Standard Calibration Curve of TFV in Tissue

Prior to measuring spatiotemporal drug distributions, a standard calibration curve was generated using homogenized drug and tissue samples to relate Raman spectral intensities to known, absolute concentrations of TFV. Freshly excised rectal tissue was cleaned, and surgical scissors were used to remove excess fat and connective tissue external to the mucosa. Tissue specimens were manually homogenized using surgical scissors before being transferred to a Bead Ruptor$_{12}$ Homogenizer (Omni International, Inc). Samples were processed in the homogenizer for a total of 12 cycles (20 second homogenization, 1 minute on ice). The cool-down period was incorporated to prevent tissue damage due to overheating.

A total of 12 dilutions of TFV in tissue homogenate were prepared, ranging from 0 to 1.24 %w/w. These dosages were chosen to span (and exceed) the range of concentrations likely to be observed in tissue as delivered from a 1% TFV clinical rectal gel. Dosed tissue homogenates were mixed manually and then homogenized for 5 cycles using the protocol delineated above. Samples were then immediately transferred to the RS-OCT system for Raman spectral analysis. Five different locations were imaged for each sample in order to obtain an averaged value of concentration within the tissue sample. A Raman spectrum of pure TFV was acquired by imaging a 1 %w/w solution of TFV in alkalinized water (50 mM NaOH) and subtracting a separately acquired spectrum of control solution[10].

Processed spectra were analyzed using MATLAB R2014b (MathWorks, Natick, MA) software. The data were least-squares fit with separately-acquired spectra of TFV and rectal tissue mucosa[16]. A standard curve was established which related the spectral contribution of TFV ($\frac{AUC\,TFV}{AUC\,Tissue}$, *AUC = Area Under the Curve*) to known concentrations of TFV in a sample. A representative fit with spectral contributions of tissue and TFV is shown in Figure 1.

E. Lateral Assay

An assay was designed in which the optical axis was parallel, rather than normal, to the epithelial surface (Figure 2a). The setup consisted of a quartz capillary tube (VitroTubes, inner Ø = 2.0 mm, outer Ø = 2.4 mm) into which tissue and drug vehicle were loaded before being transferred to the RS-OCT system for analysis. The configuration of the assay is seen in Figure 2.

Prior to acquiring spatiotemporal measurements with confocal RS-OCT, snap frozen porcine rectal tissue was thawed in a water bath at 37°C. Parchment paper was applied to the basal and apical surfaces of the tissue before excision to help maintain the structural integrity of the mucosa. Tissue was then punched using a size 5 mini punch (C.S. Osborne & Co, Harrison, NJ) and loaded into a quartz capillary tube that had been pre-loaded with 5 μL of Matrigel (BD Biosciences, San Jose, CA). The addition of Matrigel mitigated gel leakage by

creating a seal between the tissue and quartz surface. The tissue was transferred to a Heracell 240 incubator and maintained at 37°C and 5% CO_2 for 5 minutes. Next, 0.02 to 0.04 mL of 1% TFV gel was applied to the apical surface of the tissue. The ends of the quartz capillary tube were sealed with wax to prevent convective flow of the TFV gel due to influx of water. Timing of the experiment began when the gel was applied to the tissue surface. The tube was transferred to an aluminum holding chamber (Figure 2b), which could be flooded with water in order to interface with the water immersion objective of the confocal RS-OCT system. The sample was maintained at physiological temperature (37°C) throughout the experiment. The quartz-tissue interface (z=0) was identified by measuring the disappearance of the quartz peak near 270 cm-1[29] as the excitation beam was scanned across the interface. Since the epithelial surface of colorectal tissue is non-uniform, it is difficult to set a baseline for the apical surface of tissue that will be exact across all z-locations. Thus, the imaging plane was set to depth of 100 μm below the quartz surface, and the gel-tissue interface (x=0) was defined with reference to this depth. In brief, the OCT subsystem was used to visualize the gel-tissue interface (x=0) at a depth of z=100 μm below the quartz surface; the location was confirmed with the confocal RS subsystem by measuring the emergence of the phenylalanine peak of tissue as the excitation beam was scanned across the interface[30]. This allowed the scanning location to be normalized with respect to a constant epithelial surface.

Raman spectra were acquired from 100 μm below the quartz surface at approximately 30 locations (2 in gel and at least 28 in tissue). Five frames of data, each with a 15-second exposure time, were acquired. The frames were averaged to produce a single Raman spectrum per spatiotemporal position. This scanning procedure was repeated 3 times; the gel-tissue interface was re-located after each scan to account for any tissue swelling or shrinkage.

Processed spectra were ordinary least-squares fit with separately acquired spectra of placebo gel, gel components (Carbopol® 947P NF, sodium carboxymethylcellulose, methyl paraben, propyl paraben, glycerol, and EDTA), rectal tissue (mucosa and lipid), and TFV. The absolute concentrations of TFV versus time and space were determined using the standard calibration curve established with homogenized samples as described above.

Results

A. Standard Calibration Curve and Raman Sensitivity

Raman spectra of TFV dilutions in tissue homogenate revealed a strong linear correlation (R^2=0.97, p<0.001) between TFV spectral contribution and absolute TFV concentration in the sample. TFV spectral contributions within each homogenized sample were relatively uniform over all 5 locations imaged (data not shown), while TFV spectral contributions between samples decreased with decreasing concentration as expected (Figure 3a). Figure 3b shows the standard curve for TFV in rectal tissue. The limit of detection (LOD) of TFV in rectal tissue was approximated as the root mean squared error of prediction (RMSEP)[16, 31]. Here, the LOD was found to be 0.06 %w/w.

B. Associating Measures by Confocal RS and OCT

The lateral orientation of the imaging path in the assay enabled confocal RS measurements at depths well beyond those attainable using a standard ‘z-scan’ setup. A representative set of spectra spanning locations up to 500 μm below the apical surface can be seen in Figure 4a. A distinct spectral shift was evident around 360 μm and corresponded to a reduction in the TFV peak intensity at 725 cm^{-1}. This appeared to indicate a distinct region of tissue that presented a barrier to the diffusion of TFV. Corresponding changes in OCT images were also evident, revealing differences in tissue morphology that were associated with changes in spectral features (Figure 4b).

The spectral and morphological images obtained on the confocal RS-OCT system corresponded well with histological analysis of porcine rectal tissue samples. These histological images revealed a single-cell layer of epithelium under which lay the stroma and a thick adipose tissue layer (Figure 5). This is structurally similar to the morphology of human rectal mucosa. Additionally, the permeability of colorectal tissue has been shown to be similar between porcine and human samples[32]. Together, this renders porcine tissue a good model for analysis of drug delivery to human rectal mucosa.

C. Spatiotemporal Profiles of TFV in Rectal Tissue

Figure 6 shows a representative spatiotemporal diffusion profile acquired using the horizontal assay setup. Spectra were acquired through the full length of the epithelium and stromal layers (0 μm ≤ × < 380 μm) and into the adipose tissue layer (x ≥ 380 μm). As noted previously, concentrations of TFV fell to negligible levels within the adipose layer. Partitioning of drug at the gel-epithelial interface was also evident, with TFV concentrations dropping from a 1.00 %w/w loading in gel to a concentration of 0.48 %w/w at the first sample point in tissue (x depth=20 μm, time=29 min). The spatiotemporal profile of TFV concentration exhibited some diffusion-like behavior, with drug concentration decreasing with distance from the source and increasing with time after application. However, across locations within 200 μm of the gel-tissue interface, concentration remained relatively invariant with distance (see Discussion).

Discussion

We have introduced a new method for analyzing the transport of drugs through a tissue medium, enabling quantitative Raman measurements at depths unattainable using a standard ‘z-scan’ geometry. Here, the optical axis is parallel to the epithelial surface rather than normal to it. We demonstrated use of this lateral assay to analyze the transport of TFV from a 1% clinical rectal gel formulation into porcine rectal mucosal tissue. Previous work has established the utility of our confocal RS-OCT system for analyzing drug concentrations with high specificity in fluid, gels, and vaginal tissue, each of which constitute important matrices in anti-HIV microbicide development, either as delivery vehicles (fluids, gels)[22, 34] or as target sites (vaginal mucosa)[16, 23]. The strong correlation between TFV absolute concentration and the corresponding TFV spectral contribution in rectal tissue homogenate (Figure 3) indicates that this technique can be applied not only for qualitative identification of TFV, but also for quantitatively specific measurements of TFV concentration in rectal

mucosa. *In vivo* rectal biopsy data in the RMP-02/MTN-006 clinical trials has shown that median TFV concentration ranges between 4 and 10 ng/mg (0.0004 and 0.001 %w/w) at 30 minutes post-application when using a 1% TFV vaginal gel formulation[35]. This is 60–150 times lower than the LOD of our methodology. However, concentrations measured from biopsies using LC-MS/MS methods represent only the mass-averaged concentration. In reality, concentrations will be much higher at superficial depths and drop off with distance from the gel delivery vehicle. Consequently, thicker biopsies may underestimate the true TFV concentration in the epithelium and stroma[8]. A recently developed pharmacokinetic model of TFV delivery to the rectum indicates expected concentrations in the rectal stroma that are well above the LOD determined for our system[8]. The method here, therefore, provides sufficient sensitivity for analysis of local TFV concentrations at physiologically-relevant levels through the full depth of rectal stroma. The expansion of this methodology to rectal tissue, which is highly susceptible to HIV infection,[2–4, 36] thus provides another tool in the analysis of drug pharmacokinetics and in design and optimization of anti-HIV microbicides.

In this study, porcine rectal mucosal tissue was used as a model for human rectal mucosa. Histological analysis (Figure 5) revealed a high structural similarity to human rectal tissue. This distinct structure contributes to the higher susceptibility to infection of rectal vs. vaginal mucosal tissues. Unlike vaginal tissue, which consists of a thick, stratified squamous epithelial cell layer[17], rectal mucosa has only a single-cell layer of columnar epithelium which is 6 to 8 fold thinner than the vaginal epithelial layer. While this makes it more permeable to hydrophilic drugs such as TFV, it also provides less of a barrier to virion entry than vaginal mucosa[8, 19]. Beneath the epithelial layer lies the stroma, populated with a host of infectable immune cells[2, 19]. Underneath the stroma lies an adipose tissue layer along with the submucosa; these layers, too, may contain infectable immune cells[37].

This assay, for the first time, enabled Raman spectroscopic acquisition from the mucosal surface, through the full length of stroma, and into this adipose tissue layer. For porcine samples, that layer was seen to begin 380 – 1000 μm below the mucosal surface. Acquisition of confocal RS data from these depths is generally not possible due to scattering in the overlying tissues[16, 34]. Using this new lateral assay, we were able to visualize a significant drug partitioning effect at the stromal-adipose layer interface. It is likely that the presence of a thick, hydrophobic, adipose tissue layer in rectal tissue presents a barrier to hydrophilic drug diffusion, as was evident both in qualitative observation of the spectra (Figure 4a) and in quantitative analysis of concentration (Figure 6). This could have both pharmacokinetic and pharmacodynamic implications, since tenofovir transport to regions within and beyond this adipose layer would be diminished. To the extent that infectable cells lie within them, this would reduce protection against their infection by HIV virions, provided they can enter and transit the adipose layer.

Another notable transport feature evident in the TFV concentration profiles (Figure 6) was the relative invariance of concentrations across distances near the surface. While TFV concentrations did decrease with distance from the surface and increase with time at locations past 200 μm, more superficial locations (0 – 200 μm) revealed a relatively flat concentration profile. This could have been due to structural damage to the tissue surface.

The rectal tissue utilized in this experiment was snap frozen in liquid nitrogen after harvesting and then thawed prior to testing. Such procedures have a relatively small effect on drug permeation of vaginal and cervical mucosal tissue[38–40]. However, here, it is possible that such processing did damage to the superficial tissue structure[41]. This would increase drug permeability in that region. Thus, further studies of drug permeation in rectal tissue should be conducted with freshly harvested specimens.

Demonstration of this new method was conducted using the leading anti-HIV microbicide TFV. However, the suitability of this technique must be established on a case by case basis for each analyte of interest and may not be compatible with all drugs. Most importantly, for a drug to be detectable using this technique, it must present in tissue at concentrations high enough to be distinct from tissue and solvent bands[10]. We also note that, while this method does account for the spatiotemporal variability of drug concentration, it does so in 1D. Measurements can only be taken at a single spatial location per time point. Additionally, in order to achieve sufficient sensitivity, each measurement spanned a period of 75 seconds (5 frames, 15 seconds each), during which time diffusion is still occurring. In the formal computation of diffusion coefficients, this would need to be taken into account[23]. Fluorescence recovery after photobleaching (FRAP) is capable of imaging diffusion within a plane rather than at discrete points, and has been used to determine the diffusion coefficient for 2D and even 3D models of diffusion[42, 43]. However, this technique requires the conjugation of fluorescent tags to the molecule of interest. This could change its size and, therefore, its diffusion behavior. Further, FRAP is limited to measurement of diffusion over relatively small length scales, i.e. of the order of 10 μm[44]. Diffusion rates in structured media may be different over those scales and the larger one that is biologically relevant here. Finally, the photobleaching process and the related increase in temperature can damage tissue samples and impact diffusion measurements, making it less attractive in applications such as the one presented in this study.

Overall, this study provides initial proof of concept for the utility of this assay in analyzing drug transport through the full depth of excised tissue samples. Imaging with confocal RS-OCT in our previous experiments was limited to a maximal depth of 300 μm in tissue[16]. This penetration depth could be less in highly scattering tissue samples or in experiments which include an overlayer of gel on tissue (for example, real time diffusion experiments) [34]. Previously, that limitation restricted the applicability of confocal RS-OCT techniques to transparent, low scattering microbicide drug vehicles. However, anti-HIV drugs currently exist in a wide variety of delivery forms including enema, suppository, gel (opaque and transparent), film, ring, and fast dissolving insert[45–47]. The optical properties of a majority of these are incompatible with Raman analysis using a ‘z-scan’ configuration. This new assay would not only allow scans to be completed through the full length of tissue, but would be compatible with opaque and solid delivery forms of Raman visible drugs. The spatial and temporal specificity of the confocal RS-OCT system, as applied in this assay, could then be utilized to obtain drug transport parameters (i.e. diffusion and partition coefficients) both within and between the drug vehicle and tissue surface and also within and between the different layers of tissue. In conjunction with deterministic computational modeling that inputs these parameters, such information can contribute to improved microbicide product design and optimization[5, 6].

Conclusion

We successfully developed and applied a laterally oriented imaging path assay for obtaining temporally and spatially specific measures of TFV concentration throughout the full depth of excised rectal mucosal tissue. Confocal RS and OCT revealed structural differentiation of the mucosal and adipose tissue layers, while Raman spectral analysis revealed a significant tenofovir partitioning effect at this layer boundary. The information gathered from this assay highlights its utility in analyzing transport of microbicides through tissue and is not limited by light scattering that prevents deep tissue measurements using ‘z-scans’. Its potential for delineating fundamental transport parameters of microbicides from a variety of delivery forms renders this assay an asset in the development of anti-HIV microbicides.

Acknowledgments

We are grateful to Mrs. Jennifer Peters, Mr. Michael DeSoto, and Dr. Marcus Henderson (Duke University, Department of Biomedical Engineering) for their technical assistance and insight in this project. This work was supported by the National Institutes of Health [AI13127].

References

1. Neves Jd, Sarmento B. Drug delivery and development of anti-HIV microbicides: Pan Stanford 2014
2. McGowan I. Rectal microbicides: a new focus for HIV prevention. Sexually transmitted infections. 2008; 84(6):413–7. [PubMed: 19028937]
3. McGowan I, Cranston RD, Duffill K, Siegel A, Engstrom JC, Nikiforov A, et al. A phase 1 randomized, open label, rectal safety, acceptability, pharmacokinetic, and pharmacodynamic study of three formulations of tenofovir 1% gel (the CHARM-01 Study). PLoS One. 2015; 10(5):e0125363. [PubMed: 25942472]
4. Leynaert B, Downs AM, de Vincenzi I. HIV ESGoHTo. Heterosexual transmission of human immunodeficiency virus: variability of infectivity throughout the course of infection. American journal of epidemiology. 1998; 148(1):88–96. [PubMed: 9663408]
5. Katz DF, Gao Y, Kang M. Using modeling to help understand vaginal microbicide functionality and create better products. Drug delivery and translational research. 2011; 1(3):256–76. [PubMed: 22545245]
6. Katz DF, Yuan A, Gao Y. Vaginal drug distribution modeling. Advanced drug delivery reviews. 2015; 92:2–13. [PubMed: 25933938]
7. Gao Y, Katz DF. Multicompartmental pharmacokinetic model of tenofovir delivery by a vaginal gel. PLoS One. 2013; 8(9):e74404. [PubMed: 24040241]
8. Gao Y, Katz DF. Multicompartmental Pharmacokinetic Model of Tenofovir Delivery to the Rectal Mucosa by an Enema. PloS One. 2017; 12(1):e0167696. [PubMed: 28114388]
9. Gao Y, Yuan A, Chuchuen O, Ham A, Yang KH, Katz DF. Vaginal deployment and tenofovir delivery by microbicide gels. Drug Deliv Transl Res. 2015; 5(3):279–94. [PubMed: 25874971]
10. Chuchuen O, Henderson MH, Sykes C, Kim MS, Kashuba AD, Katz DF. Quantitative analysis of microbicide concentrations in fluids, gels and tissues using confocal Raman spectroscopy. PLoS One. 2013; 8(12):e85124. [PubMed: 24386455]
11. Abdool Karim Q, Abdool Karim SS, Frohlich JA, Grobler AC, Baxter C, Mansoor LE, et al. Effectiveness and safety of tenofovir gel, an antiretroviral microbicide, for the prevention of HIV infection in women. Science. 2010; 329(5996):1168–74. [PubMed: 20643915]
12. Nel AM, Coplan P, Smythe SC, McCord K, Mitchnick M, Kaptur PE, et al. Pharmacokinetic Assessment of Dapivirine Vaginal Microbicide Gel in Healthy, HIV-Negative Women. Aids Research and Human Retroviruses. 2010; 26(11):1181–90. [PubMed: 20854207]

13. Hendrix CW, Chen BA, Guddera V, Hoesley C, Justman J, Nakabiito C, et al. MTN-001: randomized pharmacokinetic cross-over study comparing tenofovir vaginal gel and oral tablets in vaginal tissue and other compartments. PLoS One. 2013; 8(1):e55013. [PubMed: 23383037]
14. Schwartz JL, Rountree W, Kashuba AD, Brache V, Creinin MD, Poindexter A, et al. A multi-compartment, single and multiple dose pharmacokinetic study of the vaginal candidate microbicide 1% tenofovir gel. PLoS One. 2011; 6(10):e25974. [PubMed: 22039430]
15. Gao Y, Yuan A, Katz DF. Tenofovir Diphosphate Concentrations in Human Vaginal Stroma after Different Dosage Regimens with a Vaginal Gel: A Modeling Approach. AIDS research and human retroviruses. 2014; 30(S1):A258–A9.
16. Maher JR, Chuchuen O, Henderson MH, Kim S, Rinehart MT, Kashuba AD, et al. Co-localized confocal Raman spectroscopy and optical coherence tomography (CRS-OCT) for depth-resolved analyte detection in tissue. Biomed Opt Express. 2015; 6(6):2022–35. [PubMed: 26114026]
17. Squier CA, Mantz MJ, Schlievert PM, Davis CC. Porcine vagina ex vivo as a model for studying permeability and pathogenesis in mucosa. Journal of pharmaceutical sciences. 2008; 97(1):9–21. [PubMed: 17721937]
18. Patton DL, Thwin SS, Meier A, Hooton TM, Stapleton AE, Eschenbach DA. Epithelial cell layer thickness and immune cell populations in the normal human vagina at different stages of the menstrual cycle. American journal of obstetrics and gynecology. 2000; 183(4):967–73. [PubMed: 11035348]
19. Hussain L, Lehner T. Comparative investigation of Langerhans' cells and potential receptors for HIV in oral, genitourinary and rectal epithelia. Immunology. 1995; 85(3):475. [PubMed: 7558138]
20. Akil A, Devlin B, Cost M, Rohan LC. Increased dapivirine tissue accumulation through vaginal film codelivery of dapivirine and tenofovir. Molecular pharmaceutics. 2014; 11(5):1533–41. [PubMed: 24693866]
21. Balázs B, Sipos P, Danciu C, Avram S, Soica C, Dehelean C, et al. ATR-FTIR and Raman spectroscopic investigation of the electroporation-mediated transdermal delivery of a nanocarrier system containing an antitumour drug. Biomedical optics express. 2016; 7(1):67–78. [PubMed: 26819818]
22. Chuchuen O, Maher JR, Simons MG, Peters JJ, Wax AP, Katz DF. Label-Free Measurements of Tenofovir Diffusion Coefficients in a Microbicide Gel Using Raman Spectroscopy. Journal of Pharmaceutical Sciences. 2017; 106(2):639–44. [PubMed: 27837968]
23. Chuchuen O, Maher JR, Henderson MH, Desoto M, Rohan LC, Wax A, et al. Label-free analysis of tenofovir delivery to vaginal tissue using co-registered confocal Raman spectroscopy and optical coherence tomography. PloS one. 2017; 12(9):e0185633. [PubMed: 28961280]
24. Fonner VA, Dalglish SL, Kennedy CE, Baggaley R, O'reilly KR, Koechlin FM, et al. Effectiveness and safety of oral HIV preexposure prophylaxis for all populations. AIDS (London, England). 2016; 30(12):1973.
25. AIDSinfoTenofovir (microbicide) [Web] US Department of Health and Human Services; 2017 [updated May 2, 2017. Available from: https://aidsinfo.nih.gov/drugs/272/tenofovir--microbicide/0/professional
26. Bitterman W, Spencer RJ, Huizenga KA, Shorter RG. Contact pH of rectal mucosa in humans and dogs. Diseases of the Colon & Rectum. 1969; 12(2):96–8. [PubMed: 5774854]
27. Hiruy H, Fuchs EJ, Marzinke MA, Bakshi RP, Breakey JC, Aung WS, et al. A phase 1 randomized, blinded comparison of the pharmacokinetics and colonic distribution of three candidate rectal microbicide formulations of tenofovir 1% gel with simulated unprotected sex (CHARM-02). AIDS research and human retroviruses. 2015; 31(11):1098–108. [PubMed: 26227279]
28. McGowan I. Rectal microbicide development. Current Opinion in HIV and AIDS. 2012; 7(6)
29. Krishnan R. Raman spectrum of quartz. Nature. 1945; 155(3937):452.
30. De Gelder J, De Gussem K, Vandenabeele P, Moens L. Reference database of Raman spectra of biological molecules. Journal of Raman Spectroscopy. 2007; 38(9):1133–47.
31. Berger AJ, Feld MS. Analytical method of estimating chemometric prediction error. Applied spectroscopy. 1997; 51(5):725–32.

32. Nejdfors P, Ekelund M, Jeppsson B, Weström BR. Mucosal in vitro permeability in the intestinal tract of the pig, the rat, and man: Species- and region-related differences. Scandinavian Journal of Gastroenterology. 2000; 35(5):501–7. [PubMed: 10868453]
33. Bergholt MS, Zheng W, Ho KY, Teh M, Yeoh KG, So JBY, et al. Fiber-optic Raman spectroscopy probes gastric carcinogenesis in vivo at endoscopy. Journal of biophotonics. 2013; 6(1):49–59. [PubMed: 23288709]
34. Chuchuen O. Development and application of Raman spectroscopy-based assays for transport analysis of anti-HIV microbicides in gels and tissues. 2015
35. Yang K-H, Hendrix C, Bumpus N, Elliott J, Tanner K, Mauck C, et al. A multi-compartment single and multiple dose pharmacokinetic comparison of rectally applied tenofovir 1% gel and oral tenofovir disoproxil fumarate. PloS One. 2014; 9(10):e106196. [PubMed: 25350119]
36. Vitinghoff E, Douglas J, Judon F, McKiman D, MacQueen K, Buchinder SP. Per-contact risk of human immunodificiency virus tramnsmision between male sexual partners. American journal of epidemiology. 1999; 150(3):306–11. [PubMed: 10430236]
37. Preza GC, Tanner K, Elliott J, Yang OO, Anton PA, Ochoa M-T. Antigen-presenting cell candidates for HIV-1 transmission in human distal colonic mucosa defined by CD207 dendritic cells and CD209 macrophages. AIDS research and human retroviruses. 2014; 30(3):241–9. [PubMed: 24134315]
38. Van der Bijl P. Effect of freezing on the permeability of human buccal and vaginal mucosa 1998
39. Gupta P, Ratner D, Patterson BK, Kulka K, Rohan LC, Parniak MA, et al. Use of Frozen–Thawed Cervical Tissues in the Organ Culture System to Measure Anti-HIV Activities of Candidate Microbicides. AIDS Research & Human Retroviruses. 2006; 22(5):419–24. [PubMed: 16706618]
40. Zidan AS, Habib MJ. Maximized mucoadhesion and skin permeation of anti-AIDS-loaded niosomal gels. J Pharm Sci. 2014; 103(3):952–64. [PubMed: 24464823]
41. McGowan I, Tanner K, Elliott J, Ibarrondo J, Khanukhova E, McDonald C, et al. Nonreproducibility of “snap-frozen” rectal biopsies for later use in ex vivo explant infectibility studies. AIDS research and human retroviruses. 2012; 28(11):1509–12. [PubMed: 22831398]
42. Deschout H, Raemdonck K, Demeester J, De Smedt SC, Braeckmans K. FRAP in pharmaceutical research: practical guidelines and applications in drug delivery. Pharmaceutical research. 2014; 31(2):255–70. [PubMed: 24019022]
43. Seiffert S, Oppermann W. Systematic evaluation of FRAP experiments performed in a confocal laser scanning microscope. Journal of microscopy. 2005; 220(1):20–30. [PubMed: 16269060]
44. Geonnotti AR, Furlow MJ, Wu T, DeSoto MG, Henderson MH, Kiser PF, et al. Measuring macrodiffusion coefficients in microbicide hydrogels via postphotoactivation scanning. Biomacromolecules. 2008; 9(2):748–51. [PubMed: 18193840]
45. Shattock RJ, Rosenberg Z. Microbicides: topical prevention against HIV. Cold Spring Harbor perspectives in medicine. 2012; 2(2):a007385. [PubMed: 22355798]
46. Nunes R, Sarmento B, das Neves J. Formulation and delivery of anti-HIV rectal microbicides: advances and challenges. Journal of Controlled Release. 2014; 194:278–94. [PubMed: 25229988]
47. Guilamo-Ramos V, Reading M, Bowman AS, Perlman DC, Barrett S. Multipurpose Prevention Technologies: A Global Sexual and Reproductive Health Priority. Journal of the Association of Nurses in AIDS Care. 2017

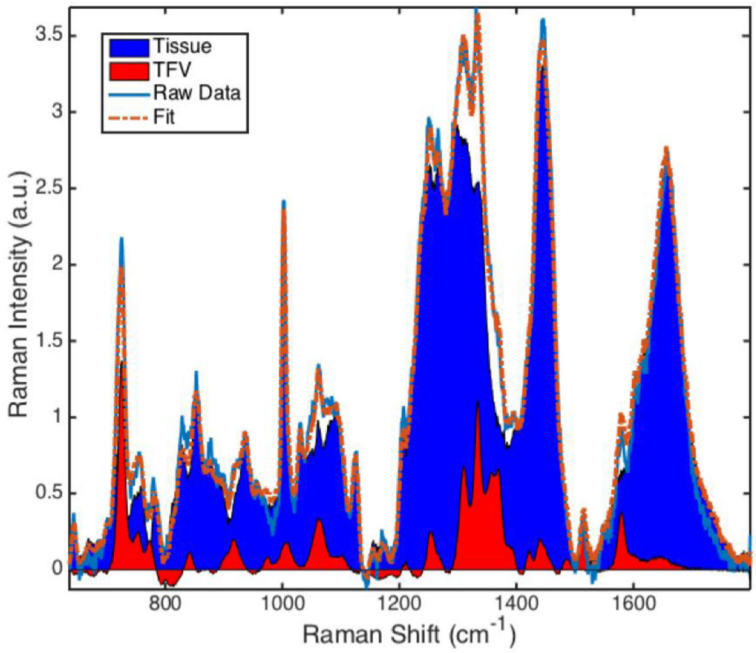

Figure 1.

Representative least-squares fit of TFV-dosed tissue homogenate (1.24 %w/w). The spectral contributions of tissue (blue) and TFV (red) can be visualized and quantitatively analyzed, allowing the relative spectral contribution of TFV to be computed as $\frac{AUC\,TFV}{AUC\,Tissue}$; AUC = Area Under the Curve.

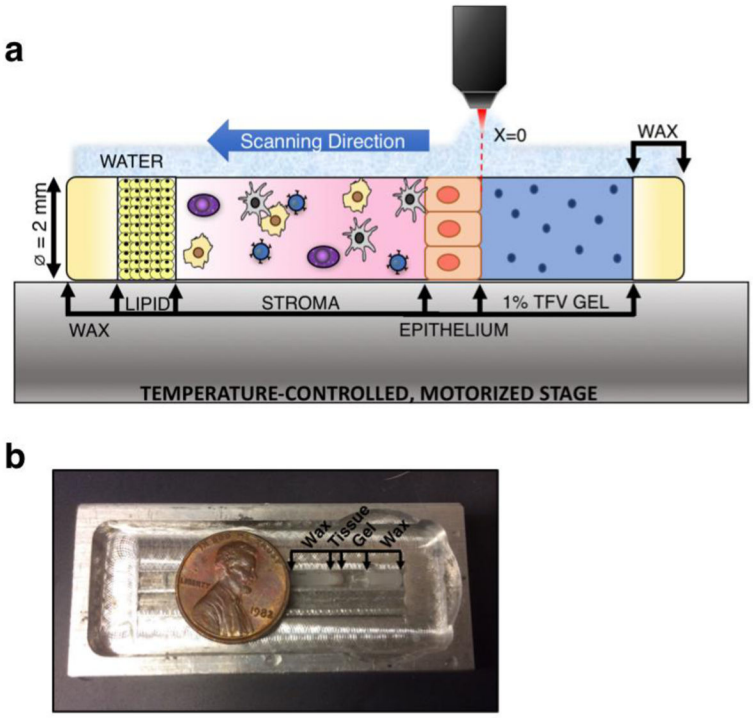

Figure 2.

a) Depiction of the lateral assay and **b)** aluminum holding chamber for interface with the water immersion objective; penny is shown for scale. Tissue was placed inside a 2.0 mm diameter quartz capillary tube, dosed with gel, and the ends sealed with wax. The prepared sample was then placed in an aluminum holding chamber, flooded with water, and transferred to the temperature-controlled, motorized stage for imaging with the confocal RS-OCT system. Scanning was conducted from the apical tissue surface through to the adipose tissue (lipid) layer that follows the stroma. All data points were taken at the same depth from the quartz surface. The horizontal coordinate location x=0 was defined as the tissue-gel interface.

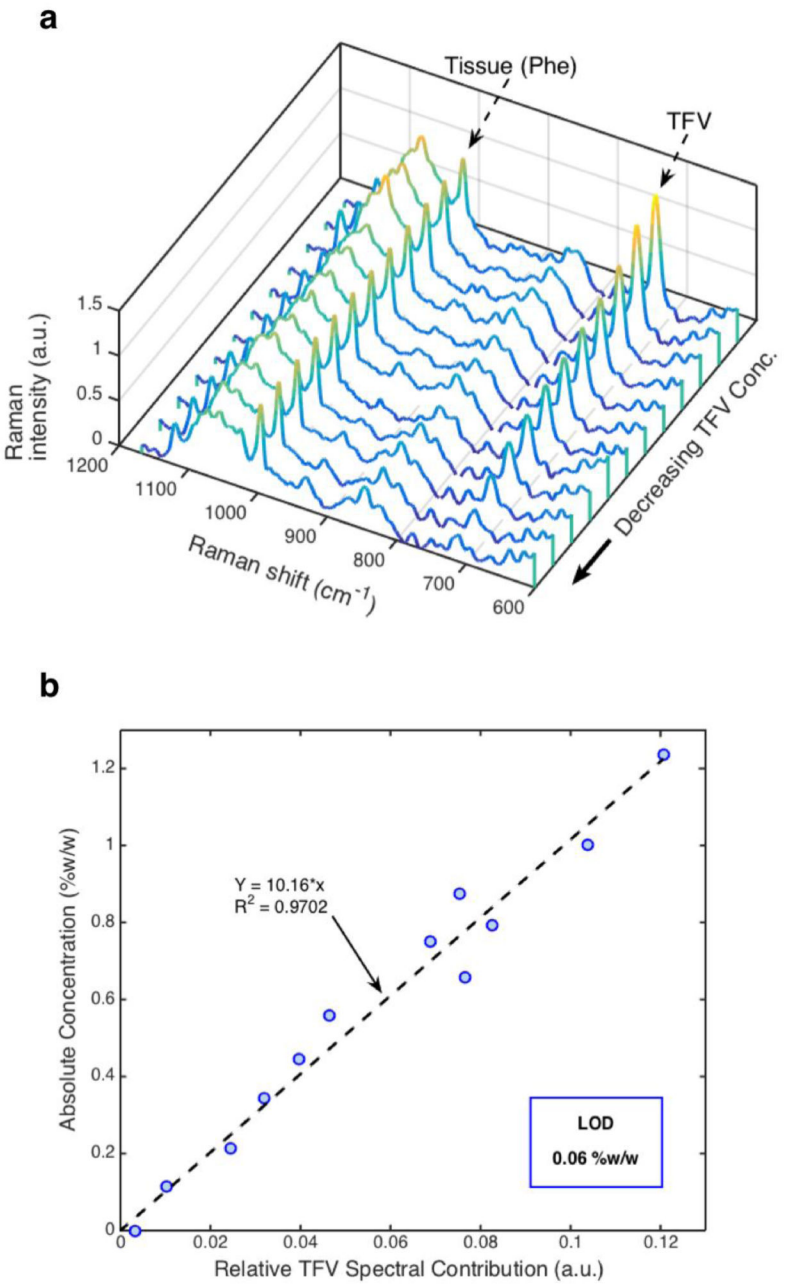

Figure 3.

a) TFV spectral peak at 725 cm^{-1} in tissue (TFV) decreased with decreasing concentration, while tissue contribution remained relatively constant as seen by the intensity of the phenylalanine peak at 1000 cm^{-1} (Phe). **b)** Raman determined concentrations of TFV were strongly, linearly correlated with absolute concentration of TFV in homogenized rectal tissue (R^2 = 0.97, p<0.001). From the root mean squared error of prediction, the limit of detection (LOD) was determined to be 0.06 %w/w for this prediction model. The standard curve was determined as Y=10.16*x; Y=absolute concentration, x=relative TFV spectral contribution

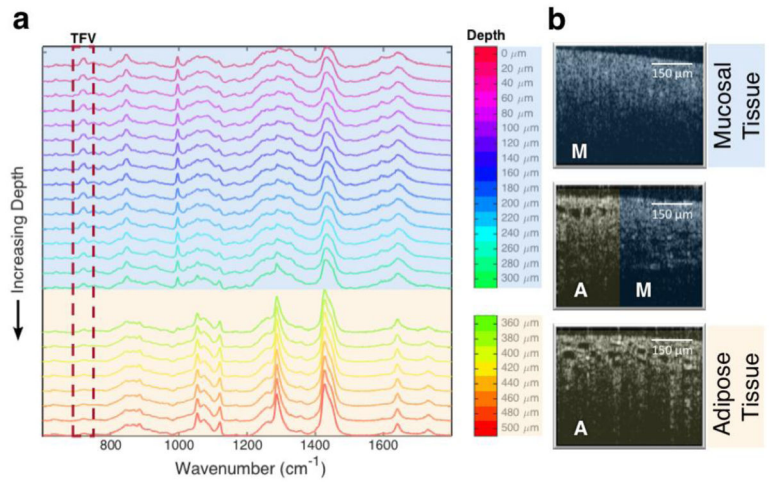

Figure 4.

a) Raman spectra at increasing depths into tissue. TFV contributions are visible at the 725 cm^{-1} peak (boxed) and were seen to drop to negligible levels beyond 360 μm. Spectra beyond 360 μm corresponded to Raman shifts characteristic of lipid[33]. **b)** The change in spectral trace correlated to a change in tissue morphology observable with OCT. A=adipose tissue, M=mucosal tissue (epithelium and stroma).

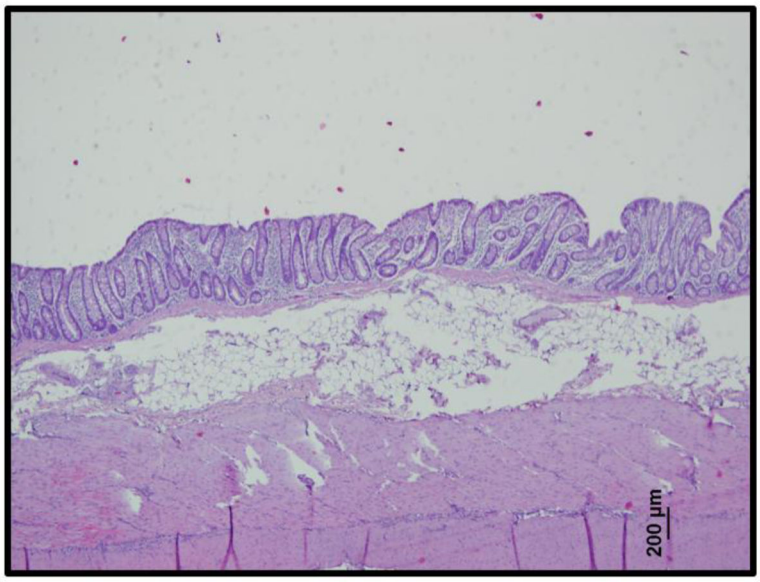

Figure 5.

Histological analysis of porcine rectal tissue (H&E stain) revealed a single-cell layer of columnar epithelium under which lay the stroma and a thick layer of adipose tissue. This corresponds well with the Raman spectra and OCT images shown in Figure 4.

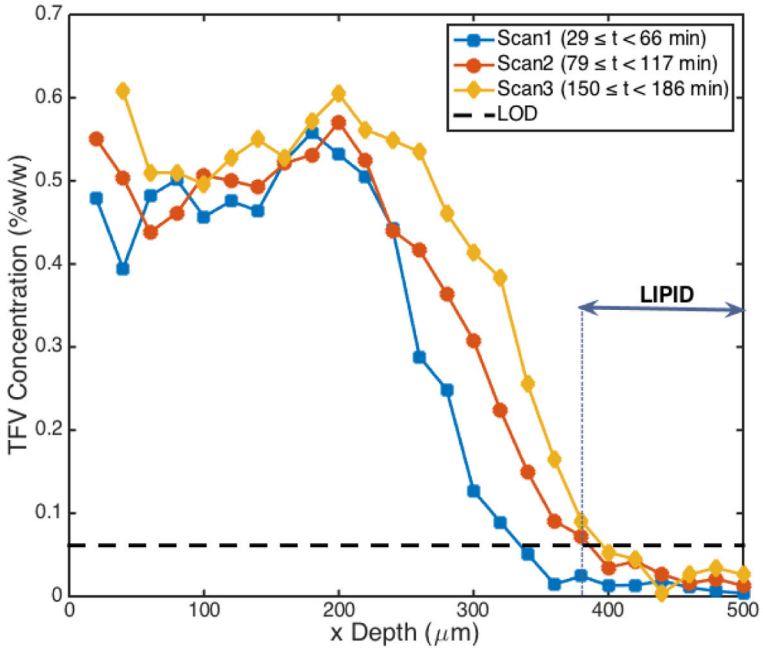

Figure 6.

Real-time TFV concentration profiles taken at increasing depths into tissue. As anticipated, concentration decreased with distance from the gel interface (x=0 μm) and increased with time (Scan 1 < Scan 2 < Scan 3). TFV concentration dropped to negligible levels within the lipid layer (x ≥ 380 μm). Of note, there was also a region of relatively invariant concentration between 0 and 200 μm.